

Granular column collapse on slope: Effect of permeability on the runout characteristics

Krishna Kumar, Jean-Yves Delenne, Kenichi Soga

Abstract: This paper investigates the effect of permeability on the runout characteristics of collapse of granular columns on slopes in fluid. Two-dimensional sub-grain scale numerical simulations are performed to understand the flow dynamics of granular collapse in fluid. The Discrete Element (DEM) technique is coupled with the Lattice Boltzmann Method (LBM), for fluid-grain interactions, to understand the evolution of submerged granular flows. The fluid phase is simulated using Multiple-Relaxation-Time LBM (LBM-MRT) for numerical stability. In order to simulate interconnected pore space in 2D, a reduction in the radius of the grains (hydrodynamic radius) is assumed during LBM computations. The collapse of granular column in fluid is compared with the dry cases to understand the effect of fluid on the runout behaviour. A parametric analysis is performed to assess the influence of the granular characteristics (initial packing) on the evolution of flow and run-out distances for slope angles of 5° . In order to understand the effect of permeability on granular flow down a slope angle of 5° , the collapse of a granular column with an initial aspect ratio of 0.8 is simulated with different permeabilities. The hydrodynamic radius of a loosely packed granular column is varied from $r = 0.7 R$ (high permeability), $0.75 R$, $0.8 R$, $0.85 R$ to $0.9 R$ (low permeability). The granular flow dynamics is investigated by analysing the effect of hydroplaning, water entrainment and viscous drag on the granular mass. The mechanism of energy dissipation, shape of the flow front, water entrainment and evolution of packing density is used to explain the difference in the flow characteristics of granular column collapse in fluid.

1 Introduction

Catastrophic earth movement events, such as landslides, debris flows, rock avalanches and reservoir embankment failures, exemplify the potential consequences of an earth gravitational instability. Slope failure is a problem of high practical importance for both civil engineering structures and natural hazard management. The study described in this paper examines the stability of underwater slopes, which are caused by excess seepage or earthquakes. They can damage offshore structures nearby and may generate a tsunami.

In order to describe the mechanism of underwater granular flows, it is necessary to consider both the dynamics of the solid phase of granular matter and the role of the ambient fluid, which exists

either inside the pores of the granular body and as free water outside the granular body (Denlinger and R. Iverson, 2001; R. M. Iverson, 1997). Initial acceleration plays a crucial role in underwater landslide propagation (Romano et al., 2017), as the initial acceleration increases, there is a limited time for the landslide to deform during the acceleration phase. The initiation and propagation of submarine granular flows depend mainly on geometry (e.g. slope angle, lateral extent, etc), initial stress conditions, density, soil properties, and the quantity of the material destabilised. Although certain macroscopic models are capable of capturing simple mechanical behaviour (e.g. Topin et al. (2011)), the complex fundamental mechanism that occurs at the grain scale, such as hydrodynamic instabilities, the formation of clusters, collapse, and transport, require further investigation in order to make better engineering assessment of the potential risk of damages against underwater slope failures for example.

The momentum transfer between the discrete and the continuous phases of fluid saturated granular material significantly affects the dynamics of the flow (Peker and Helvaci, 2007). The grain-scale description of the granular material enriches the macro-scale variables. In particular, when the solid phase reaches a high-volume fraction, it is important to consider the strong heterogeneity arising from the contact forces between the grains, the drag interactions which counteract the movement of the grains, and the hydrodynamic forces that reduce the weight of the grains inducing a transition from a dense compacted to a dense suspended flow (Meruane, Tamburrino, and Roche, 2010).

The case of granular material movements in presence of an interstitial fluid at the grain-scale has been less studied. In this paper, we report the findings of the study on the granular column collapse in fluid in the inclined configuration using the coupled Lattice Boltzmann Method (LBM) and Discrete Element Method (DEM). We examined the effect of density and slope angle on the runout evolution.

The Lattice Boltzmann Method is a ‘micro-particle’ based numerical time-stepping procedure for the solution of incompressible fluid flows. Consider a 2D incompressible fluid flow with density ρ and kinematic viscosity ν , in a rectangular domain D . The fluid domain is divided into a rectangular grid or lattice, with the same spacing ‘ h ’ in both the x - and the y -directions, as shown in fig. 1. The present study focuses on two-dimensional problems, hence the $D2Q9$ momentum discretisation is adopted (see (He et al., 1997) for naming convention).

The lattice Boltzmann Bhatnagar-Gross-Krook (LGBK) method is capable of simulating various hydrodynamics (Succi, 2001) and offers intrinsic parallelism. Although LBM is successful in modelling complex fluid systems, such as multiphase flows and suspensions in fluid, the LBM may lead to numerical instability when the dimensionless relaxation time τ is close to 0.5. The Multi-Relaxation Time Lattice Boltzmann Method (LBM-MRT) overcomes the deficiencies of linearised single relaxation LBM-BGK, such as fixed Prandtl number ($Pr=\nu/\kappa$), where the thermal conductivity ‘ κ ’ is unity (Liu, Sun, and Wang, 2003). The LB-MRT model offers better numerical stability and has more degrees of freedom. In the formulation of the linear Boltzmann equation with multiple relaxation time approximation, the lattice Boltzmann equation is written as:

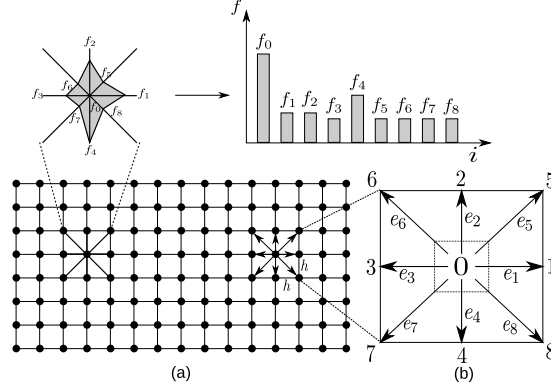


Figure 1: The Lattice Boltzmann discretisation and D2Q9 scheme: (a) a standard LB lattice and histogram views of the discrete single particle distribution function/direction-specific densities f_i ; (b) D2Q9 model

$$\begin{aligned} f_\alpha(\mathbf{x} + \mathbf{e}_i \Delta_t, t + \Delta_t) - f_\alpha(\mathbf{x}, t) \\ = -\mathbf{S}_{\alpha i}(f_i(\mathbf{x}, t) - f_i^{eq}(\mathbf{x}, t)) \end{aligned} \quad (1)$$

where \mathbf{S} is collision matrix. The nine eigen values of \mathbf{S} are all between 0 and 2 so as to maintain linear stability and the separation of scales, which means that the relaxation times of non-conserved quantities are much faster than the hydrodynamic time scales. The LGBK model is the special case in which the nine relaxation times are all equal and the collision matrix $\mathbf{S} = \frac{1}{\tau} \mathbf{I}$, where \mathbf{I} is the identity matrix. The evolutionary progress involves two steps, advection and flux. The advection can be mapped to the momentum space by multiplying through by a transformation matrix \mathbf{M} and the flux is still finished in the velocity space. The evolutionary equation of the multi-relaxation time lattice Boltzmann equation is written as:

$$\begin{aligned} \mathbf{f}(\mathbf{x} + \mathbf{e}_i \Delta_t, t + \Delta_t) - \mathbf{f}(\mathbf{x}, t) \\ = -M^{-1} \hat{\mathbf{S}}(\hat{\mathbf{f}}(\mathbf{x}, t) - \hat{\mathbf{f}}^{eq}(\mathbf{x}, t)) \end{aligned} \quad (2)$$

where \mathbf{M} is the transformation matrix mapping a vector \mathbf{f} in the discrete velocity space $\mathbb{V} = \mathbb{R}^b$ to a vector $\hat{\mathbf{f}}$ in the moment space $\mathbb{V} = \mathbb{R}^b$.

$$\hat{\mathbf{f}} = \mathbf{M} \mathbf{f} \quad (3)$$

$$\mathbf{f}(\mathbf{x}, t) = [f_0(\mathbf{x}, t), f_1(\mathbf{x}, t), \dots, f_8(\mathbf{x}, t)]^T \quad (4)$$

The collision matrix $\hat{\mathbf{S}} = \mathbf{M} \mathbf{S} \mathbf{M}^{-1}$ in moment space is a diagonal matrix: $\hat{\mathbf{S}} = \text{diag}[s_1, s_2, s_3, \dots, s_9]$. The transformation matrix \mathbf{M} can be constructed via Gram-Schmidt orthogonalisation procedure.

Through the Chapman-Enskog expansion (Du, Shi, and Chen, 2006), the incompressible Navier-Stokes equation can be recovered and the viscosity is given as:

$$\nu = c_s^2 \Delta t (\tau - 0.5) \quad (5)$$

1.1 Turbulence in Lattice Boltzmann Method

Modelling fluids with low viscosity like water remains a challenge, necessitating very small values of h , and/or τ very close to 0.5 (He et al., 1997). Turbulent flows are characterised by the occurrence of eddies with multiple scales in space, time and energy. In this study, the Large Eddy Simulation (LES) is adopted to solve for turbulent flow problems. The separation of scales is achieved by filtering of the Navier-Stokes equations, from which the resolved scales are directly obtained and unresolved scales are modelled by a one-parameter Smagorinski sub-grid methodology, which assumes that the Reynold's stress tensor is dependent only on the local strain rate (Smagorinsky, 1963). The turbulent viscosity ν is related to the strain rate S_{ij} and a filtered length scale 'h' as follows:

$$v_t = (S_c h)^2 \bar{S}; \quad (6)$$

$$\bar{S} = \sqrt{\sum_{i,j} \tilde{S}_{i,j} \tilde{S}_{i,j}} \quad (7)$$

where S_c is the Smagorinski constant found to be close to 0.03 (Yu, Girimaji, and Luo, 2005).

The effect of the unresolved scale motion is taken into account by introducing an effective collision relaxation time scale τ_t , so that the total relaxation time τ_* is written as:

$$\tau_* = \tau + \tau_t \quad (8)$$

where τ and τ_t are respectively the standard relaxation times corresponding to the true fluid viscosity ν and the turbulence viscosity v_t , defined by a sub-grid turbulence model. The new viscosity v_* corresponding to τ_* is defined as:

$$v_* = \nu + v_t = \frac{1}{3}(\tau + \tau_t - \frac{1}{2})C^2 \Delta t \quad (9)$$

$$v_t = \frac{1}{3}\tau_t C^2 \Delta t \quad (10)$$

The Smagorinski model is easy to implement and the Lattice Boltzmann formulation remains unchanged, except for the use of a new turbulence-related viscosity τ_* . The component s_1 of the collision matrix becomes $s_1 = \frac{1}{\tau + \tau_t}$.

2 Coupled LB-DEM model

2.1 General

The Lattice Boltzmann approach has the advantage of accommodating large particle sizes and the interaction between the fluid and the moving particles can be modelled through relatively simple fluid - particle interface treatments. Further, employing the Discrete Element Method (DEM) to account for the particle/particle interaction naturally leads to a combined LB - DEM solution procedure. The Eulerian nature of the Lattice Boltzmann formulation, together with the common explicit time step scheme of both the Lattice Boltzmann and the Discrete Element, makes this coupling strategy an efficient numerical procedure for the simulation of particle-fluid systems (Cook, Noble, and Williams, 2004). The LB-DEM coupling system is a powerful fundamental research tool for investigating hydro-mechanical physics in porous media flow. To capture the actual physical behaviour of a fluid-particle system, the boundary condition between the fluid and the particle is modelled as a non-slip boundary condition, i.e. the fluid near the particle should have a similar velocity as the particle boundary. The solid particles inside the fluid are represented as solid lattice nodes. The discrete nature of lattice will result in stepwise representation of the surfaces (Kumar, 2015). A very small lattice spacing is adopted to obtain smoother boundaries.

The smallest DEM grain in the system controls the size of the lattice. In the present study, a very fine resolution of $d_{min}/h = 10$ is adopted. That is, the smallest grain with a diameter d_{min} in the system is discretized into 100 lattice nodes ($10h \times 10h$). This provides a very accurate representation of the interaction between the solid and the fluid nodes.

When combining the Discrete Element modelling of grain interactions with the lattice Boltzmann formulation, an issue arises. That is, there are now two time steps: Δt for the fluid flow and Δt_D for the particle movements. Since Δt_D is normally smaller than Δt , Δt_D is slightly reduced to a new value Δt_s so that Δt and Δt_s have an integer ratio n_s :

$$\Delta t_s = \Delta t / n_s \quad (11)$$

$$n_s = [\Delta t / \Delta t_D] + 1 \quad (12)$$

This results in a subcycling time integration for the Discrete Element part. Δt every step of the fluid computation, n_s sub-steps of integration are performed for DEM using the time step Δt_s . The hydrodynamic force is unchanged during this sub-cycling.

2.2 Modelling Permeability

In DEM, the grain – grain interaction is described based on the contact interactions. In a 3D granular assembly, the pore spaces between grains are interconnected, whereas in 2-D assembly,

the grains are in contact with each other that result in a non-interconnected pore-fluid space. This results in a no flow condition in a 2-D case (see fig. 2). In order to overcome this difficulty, a reduction in radius is assumed only during LBM computations (fluid and fluid–solid interaction), which is called the hydrodynamic radius. The hydrodynamic radius allows interconnected pore space through which the surrounding fluid can flow (hydrodynamic radius $r = 0.7 R$ to $0.95 R$, where ‘ R ’ is the grain radius). The hydrodynamic radius is used only during the LBM computations, and has no effect on the grain–grain interactions computed using DEM. Different values of macroscopic permeability can be obtained for any given initial packing by varying the hydrodynamic radius of the grains, without having to change the actual granular packing. This introduces a new parameter into the system. In a physical sense, a hydrodynamic radius represents the three-dimensional permeability of a granular assembly simulated as a two-dimensional geometry.

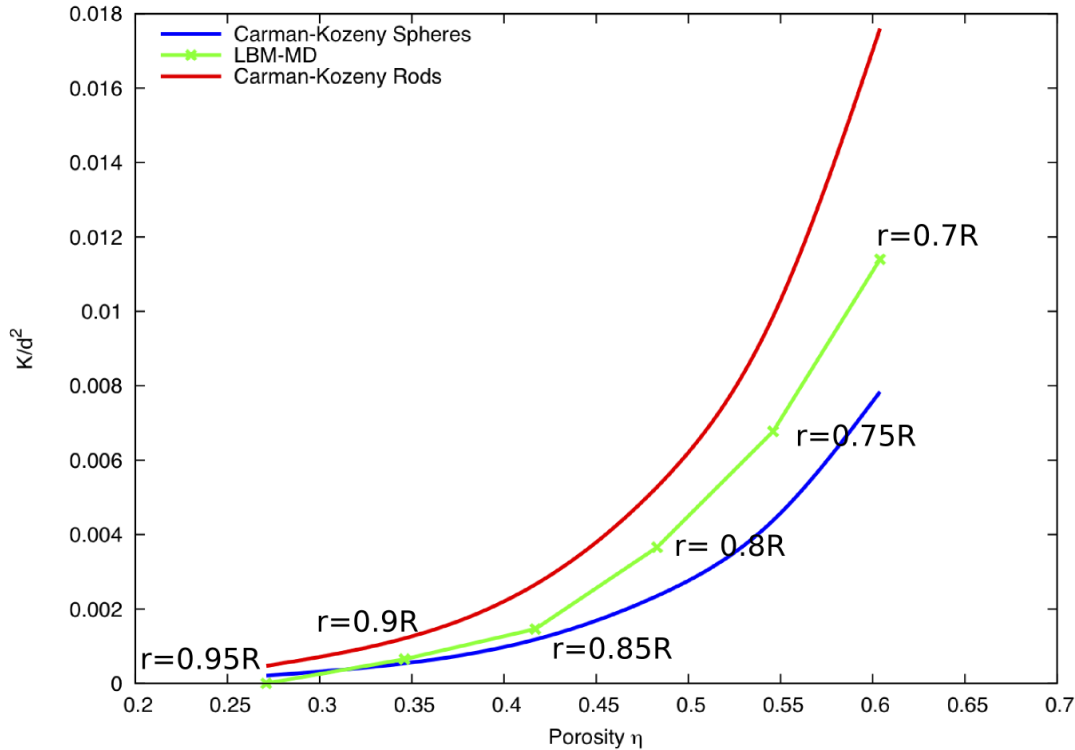


Figure 2: Relation between permeability and porosity for different hydrodynamic radius and comparison with the analytical solution.

In order to understand the relation between the hydrodynamic radius and the permeability of a granular assembly, permeability tests are performed by varying the hydrodynamic radius r as $0.7 R$, $0.75 R$, $0.8 R$, $0.85 R$, $0.9 R$ and $0.95 R$. The permeability values obtained are normalized by the square of the average grain diameter following the Carman-Kozeny equations (Yazdchi, Srivastava, and Luding, 2011). The comparison of normalised permeability from the 2D LB-DEM simulations with the Carman-Kozeny equations for spherical and cylindrical grain assembly for different porosities are presented in fig. 3. It can be observed from the figure that the permeability decreases drastically as the radius is decreased from $0.7R$ to $0.95R$. The granular assembly is almost impermeable for a hydrodynamic radius of $0.95R$. The normalized permeability is found

to match the qualitative trend of the Carman-Kozeny equations.

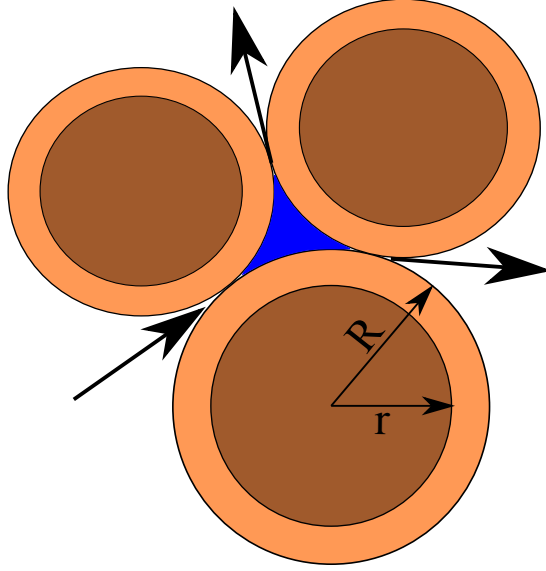


Figure 3: Schematic representation of the hydrodynamic radius in LBM-DEM computation.

3 Granular column collapse on slopes in fluid

3.1 Problem definition

In this study, a 2D polydisperse system ($d_{max}/d_{min} = 1.8$) of circular discs in fluid was used to understand the behaviour of granular flows on inclined planes. As shown in ??, an inclined gravity direction was varied to examine the slope angle effect. The soil column was modelled using 1000 discs of density 2650 kg/m^3 and a contact friction angle of 26° . The aspect ratio ‘a’ is defined as the ratio of the initial height (H_i) to the width (L_i) of the column. A granular column of aspect ratio ‘a’ of 0.8 was used. The collapse of the column was simulated inside a fluid with a density of 1000 kg/m^3 and a kinematic viscosity of $1 \times 10^{-6} \text{ m}^2/\text{s}$. The choice of a 2D geometry has the advantage of cheaper computational effort than a 3D case, making it feasible to simulate very large systems. To model 3D permeability nature of spheres as 2D discs, a reduction in radius: a hydrodynamic radius $r = 0.9R$ was adopted only for LBM computations, as described earlier. Dry column collapse was also performed to study the effect of hydrodynamic forces on the runout distance. The runout distance is normalised with respect to the initial width of the column. The granular column collapse was allowed to flow down a slopes of 5° .

References

- [1] B.K. Cook, D.R. Noble, and J.R. Williams. “A direct simulation method for particle-fluid systems”. In: *Engineering Computations* 21.2/3/4 (2004), pp. 151–168.

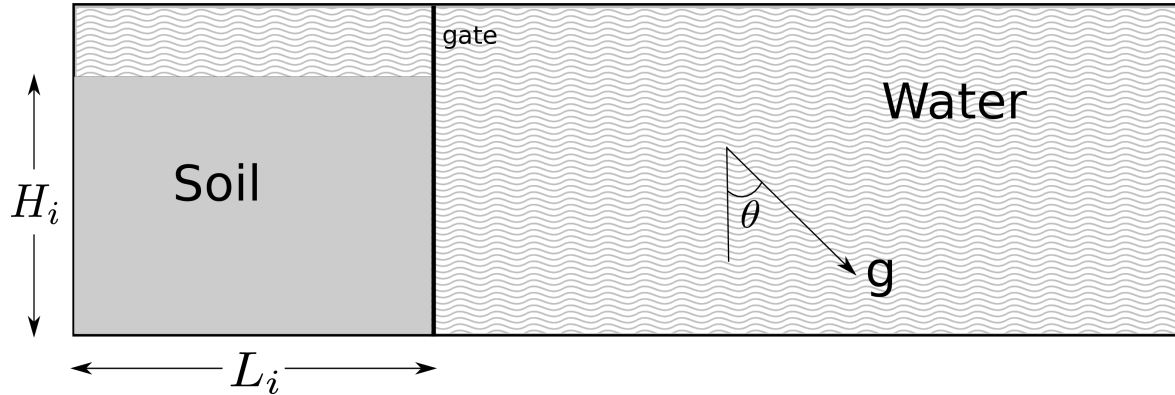


Figure 4: Underwater granular collapse set-up

- [2] R.P. Denlinger and R.M. Iverson. “Flow of variably fluidized granular masses across three-dimensional terrain, ii: Numerical predictions and experimental tests”. In: *J. Geophys. Res* 106.B1 (2001), pp. 553–566.
- [3] Rui Du, Baochang Shi, and Xingwang Chen. “Multi-relaxation-time lattice Boltzmann model for incompressible flow”. In: *Physics Letters A* 359.6 (Dec. 2006), pp. 564–572. ISSN: 03759601. DOI: 10.1016/j.physleta.2006.07.074. URL: <http://dx.doi.org/10.1016/j.physleta.2006.07.074>.
- [4] X. He et al. “Analytic solutions of simple flows and analysis of nonslip boundary conditions for the lattice Boltzmann BGK model”. In: *Journal of Statistical Physics* 87.1 (1997), pp. 115–136. URL: <http://www.springerlink.com/index/u78vx6375h7746p3.pdf>.
- [5] Richard M. Iverson. “The physics of debris flows”. In: *Rev. Geophys.* 35.3 (1997), pp. 245–296.
- [6] Krishna Kumar. “Multi-scale multiphase modelling of granular flows”. PhD thesis. University of Cambridge, 2015.
- [7] S. H. Liu, D. A. Sun, and Yisen Wang. “Numerical study of soil collapse behavior by discrete element modelling”. In: *Computers and Geotechnics* 30.Compendex (2003), pp. 399–408.
- [8] C. Meruane, A. Tamburrino, and O. Roche. “On the role of the ambient fluid on gravitational granular flow dynamics”. In: *Journal of Fluid Mechanics* 648 (2010), pp. 381–404.
- [9] S.M. Peker and S.S. Helvaci. *Solid-liquid two phase flow*. Elsevier, 2007. ISBN: 9780444522375.
- [10] Alessandro Romano et al. “3D physical modeling of tsunamis generated by submerged landslides at a conical island: the role of initial acceleration”. In: *Coastal Engineering Proceedings* 1.35 (2017), p. 14.
- [11] J. Smagorinsky. “General circulation experiments with the primitive equations”. In: *Monthly weather review* 91.3 (1963), pp. 99–164.

- [12] Sauro Succi. *The lattice Boltzmann equation for fluid dynamics and beyond*. Oxford University Press, 2001, p. 288. ISBN: 0198503989. URL: <http://books.google.com/books?hl=en&%7B%5C&%7Dlr=%7B%5C&%7Ddid=OC0Sj%7B%5C%7DxgnhAC%7B%5C&%7Dpgis=1>.
- [13] V. Topin et al. “Micro-rheology of dense particulate flows: Application to immersed avalanches”. In: *Journal of Non-Newtonian Fluid Mechanics* 166.1-2 (2011), pp. 63–72.
- [14] K. Yazdchi, S. Srivastava, and S. Luding. “Microstructural effects on the permeability of periodic fibrous porous media”. In: *International Journal of Multiphase Flow* (2011). URL: <http://www.sciencedirect.com/science/article/pii/S0301932211001005%20http://www2.msm.ctw.utwente.nl/kyazdchi/Papers/IJMF11.pdf>.
- [15] H. Yu, S.S. Girimaji, and L.S. Luo. “Lattice Boltzmann simulations of decaying homogeneous isotropic turbulence”. In: *Physical Review E* 71.1 (2005), p. 016708.

Author

Dr. Krishna Kumar
Department of Engineering
University of Cambridge
Cambridge, CB2 1PZ
Tel.: +44(0) 1223 748 589
e-mail: kks32@cam.ac.uk
Web: www.cb-geo.com